Metal Particle Growth during Glucose Hydrogenation over Ru/SiO_2 Evaluated by X-ray Absorption Spectroscopy and Electron Microscopy

Erin P. Maris,[†] William C. Ketchie,[†] Vladimir Oleshko,[‡] and Robert J. Davis*[,†]

Department of Chemical Engineering and Department of Materials Science and Engineering, University of Virginia, Charlottesville, Virginia 22904-4741

Received: December 2, 2005; In Final Form: February 21, 2006

Biorenewable resources such as carbohydrates are considered alternative feedstocks for oxygenated chemicals. This work investigates the stability of silica-supported Ru catalysts in the aqueous phase conversion of glucose to sorbitol. In situ X-ray absorption spectroscopy at the Ru K edge revealed that air-exposed silica-supported Ru was in an oxidized state but was subsequently reduced in aqueous solutions saturated with 40 bar H_2 at 373 K. Furthermore, exposure to aqueous phase conditions resulted in the sintering of Ru particles on the silica surface. However, the presence of glucose in the aqueous phase stabilized the growth of the Ru particles. Batchwise hydrogenation of glucose at 373 K and 80 bar H_2 over a Ru/SiO_2 (2.67 wt %) catalyst is nearly 100% selective to sugar alcohol with an average turnover frequency of 0.21 ± 0.04 s^{-1}. The hydrogenation reaction was not mass transfer limited according to the Madon−Boudart criterion.

Introduction

The production of fuels and chemicals relies heavily upon fossil-fuel-derived precursors that are finite in supply. Increased effort to find alternatives to these fossil-based resources has focused on species such as carbohydrates that are derived from renewable biomass. Carbohydrates can be converted to dihydrogen, alkanes, oxygenated chemicals, and other industrially important chemical intermediates.[1−12] As a first step, the simple sugar glucose can be hydrogenated to the sugar alcohol sorbitol over a transition metal catalyst (Figure 1). Sorbitol is an important intermediate used in the production of vitamin C.[12] Sorbitol can also be converted to fuels such as H_2 and alkanes by aqueous phase reforming and transformed into lower molecular weight polyols and acids through hydrogenolysis.[1,4,7,13] Hydrogenolysis products can be further converted to fuels or commodity oxygenated chemicals.[2,7]

Traditionally, the hydrogenation of glucose to sorbitol utilized nickel-based catalysts because of their low cost.[14−20] Unfortunately, leaching of nickel from these catalysts decreased hydrogenation activity and posed a separation problem in downstream processing. Efforts to find alternatives to nickel-based catalysts have resulted in the exploration of cobalt-, platinum-, palladium-, rhodium-, and ruthenium-based catalysts.[15,21−23] Materials containing Ru appear to be the most active hydrogenation catalysts, and unlike nickel, they do not appear to leach into the reaction medium.[15,21,24−26] Deactivation of the catalysts, however, can often be an issue.[25] For example, Arena investigated the hydrogenation of glucose over Ru/Al_2O_3, whereas Gallezot et al. studied a Ru/C catalyst. Both groups concluded that deactivation of the catalyst could be attributed, in part, to poisoning of the Ru surface by metal impurities in solution. Arena also found that byproduct formation and increased levels of alumina crystallinity contributed to catalyst deactivation. Furthermore, Gallezot et al. postulated that deactivation also involved sintering of Ru particles. Thus, the choice of catalyst support is crucial in the hydrogenation of glucose. Because of the inert nature of silica, ruthenium catalysts supported on silica appear to be superior to their titania-, alumina-, and carbon-supported analogues for minimizing byproduct formation.[15] However, the stability of the silica can be compromised under aqueous reaction conditions.[27] This paper focuses on the use of in situ catalyst characterization used to probe the stability of silica-supported ruthenium catalysts for the conversion of glucose to sorbitol.

Experimental Methods

Materials Preparation. Various weight loadings of ruthenium were supported on silica (Cab-O-Sil M-5, BET surface area 196 m^2 g^{-1}) by incipient wetness impregnation involving an aqueous solution of $Ru(NO)(NO_3)_3$ (Alfa-Aesar, 1.5% w/v). Approximately 4.7 mL of the impregnating solution was used per gram of silica. After impregnation, the catalysts were dried overnight under ambient conditions, followed by drying in air at 393 K for 2 h.

A carbon-supported sample (Ru/C) was prepared to be used during X-ray absorption studies evaluating the effect of support on the stability of Ru particles in an aqueous environment. The Ru/C samples were prepared by cation exchange according to the method published by Gallezot et al.[26] Prior to the ion exchange, 20 g of carbon powder (Alfa Aesar, BET surface area 665 m^2 g^{-1}) was chemically oxidized by treatment with 380 mL of aqueous sodium hypochlorite solution (Acros, 5% active chlorine) at ambient temperature. The NaClO solution was added dropwise to the carbon. The resulting slurry was stirred for approximately 24 h under ambient conditions. The mixture was subsequently filtered and washed with 250 mL of 1 M HCl (Acros) to remove Na^+. The oxidized carbon was then washed repeatedly with distilled deionized water until the filtrate tested negative for Cl^- using a 0.1 M $AgNO_3$ solution. To prepare the Ru/C sample, the oxidized carbon support was washed with 1 M aqueous ammonia solution (Alfa Aesar, 50% v/v) while bubbling N_2 through the mixture at ambient temperature. An appropriate amount of $Ru(NH_3)_6Cl_3$ (Acros) in 1

* Corresponding author. E-mail: rjd4f@virginia.edu.
[†] Department of Chemical Engineering.
[‡] Department of Materials Science and Engineering.

10.1021/jp057022y CCC: $30.25
Published on Web 03/25/2006

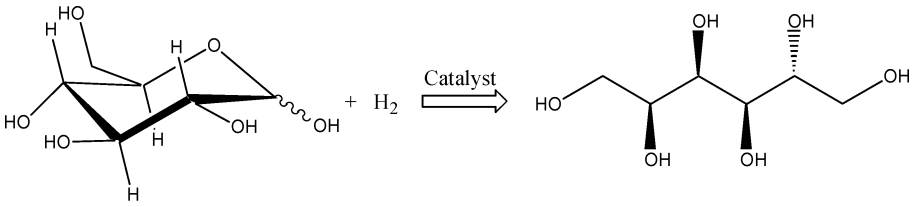

Figure 1. Reaction scheme of glucose hydrogenation to sorbitol.

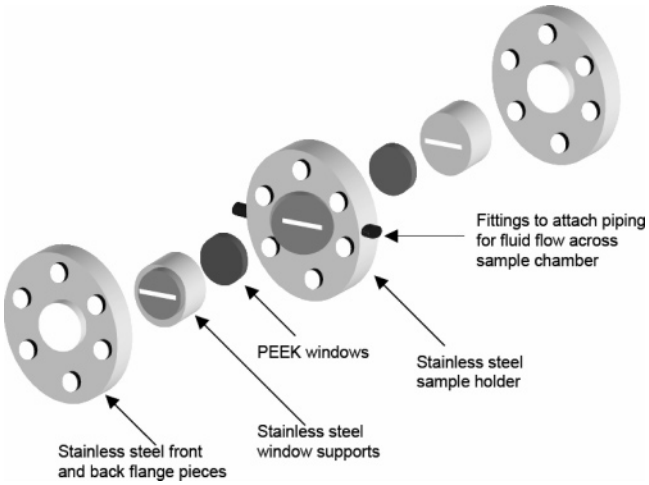

Figure 2. Schematic of the XAS sample cell.

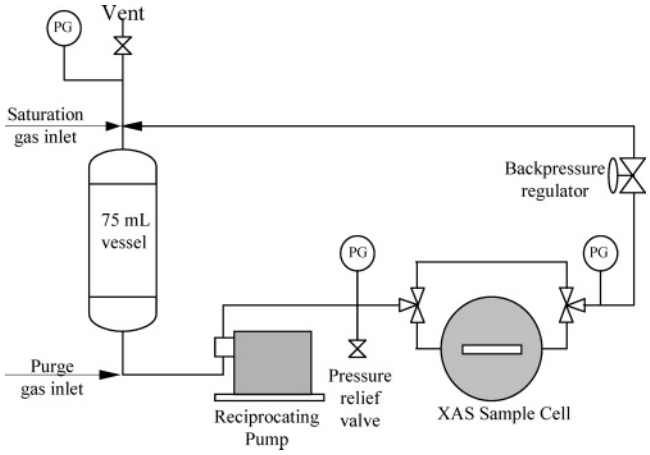

Figure 3. Schematic of the flow system and sample cell for XAS studies. "PG" denotes pressure gauge.

M aqueous ammonia solution was added dropwise to the carbon slurry. The resulting suspension was stirred at ambient temperature in the presence of bubbling N_2 for 24 h. The suspension was filtered and washed with distilled deionized water until no Cl^- could be detected with a 0.1 M $AgNO_3$ test. The sample was dried overnight under ambient conditions, followed by drying in air at 383 K for 2 h.

These materials were heated at 1 K min^{-1} in H_2 (BOC, 99.999%, purified using a Matheson 8371V palladium hydrogen purifier) flowing at 84 mL min^{-1} to 648 K and held at that temperature for 3 h. The reduced samples were then cooled under H_2 and slowly exposed to air. These will be referred to as the "as-prepared" samples. Ruthenium loading was evaluated by Galbraith Laboratories (Knoxville, TN).

An alumina-supported Ru sample was prepared for use as a reference in the X-ray absorption studies. This sample was prepared by incipient wetness impregnation of a γ-alumina support (Alfa Aesar, 99.97%, 80−120 m^2 g^{-1}) with an aqueous solution of $RuCl_3 \cdot xH_2O$ (Alfa Aesar, 41.6 wt % Ru). Following impregnation, the sample was dried in air overnight, followed by drying in air at 393 K for 2 h. Subsequently, the sample was heated in flowing H_2 to 673 K at a rate of 4 K min^{-1} and then held at 673 K for 4 h. The sample was cooled under H_2 followed by a slow exposure to air.

X-ray Absorption Spectroscopy. In situ X-ray absorption spectroscopy (XAS) studies were performed on beamline X-18B at the National Synchrotron Light Source (2.8 GeV, ring currents of 160−300 mA) at Brookhaven National Laboratory, Upton, NY. All XAS data were collected in transmission mode. A slit size of 0.3 mm × 10 mm was used which allowed for 3.5 eV resolution at the Ru K edge (22.118 keV).

An XAS sample cell similar to that found in ref 28 was constructed to allow for liquid flow across the catalyst at the elevated pressures and temperatures required for glucose hydrogenation. A schematic of the cell is shown in Figure 2. The catalyst samples (particle size 53−75 μm) were hand-pressed into the 1.5 mm × 20 mm × 3 mm (path length) sample holder. A 20 μm stainless steel frit retained the catalyst in the flowing reaction mixture. The cell windows consisted of 1 mm thick poly-ether-ether-ketone (PEEK) disks. A schematic of the flow system and sample cell setup is shown in Figure 3. The aqueous solution used as the reaction medium was first purged with N_2 and then pressurized with either N_2 or H_2 in a 75 mL vessel. A reciprocating piston pump was used to circulate the aqueous solution at a rate of 1.5 mL min^{-1}. The solution was first pumped through a recycle loop that bypassed the sample cell for 90 min to allow the solution to reach H_2 saturation before introduction to the sample. The cell was heated and maintained at 373 K using heating tape and a temperature controller. All aqueous treatments were conducted for 3 h prior to data collection.

The extended X-ray absorption fine structure (EXAFS) data analysis was performed using the WinXAS software package.[29] An average of four to six scans was used for analysis. The first-shell Ru−Ru amplitude function and phase shift were extracted from the Ru/Al_2O_3 (17.6 wt % Ru) sample. The average Ru particle size was found to be greater than 10 nm, as determined by H_2 chemisorption and X-ray diffraction (XRD). The reference sample was assumed to have the bulk crystallographic values of the Ru hexagonal close-packed (hcp) structure with a first-shell coordination number of 12 and nearest neighbor distance of 2.68 Å. The EXAFS data were k^1 and k^3 weighted and then Fourier transformed from 3 to 15.5−16.0 $Å^{-1}$. Next, the Fourier transforms were back-transformed over the first Ru−Ru shell in *R*-space from 1.3 to 3.1 Å. Curve fitting was performed in both *R*-space and *k*-space with k^1 and k^3 weighting, and the average of these four values is reported herein. This procedure results in an estimated accuracy within 10% for the coordination number, ±10% for the Debye−Waller factor, and ±0.01 Å for the interatomic distance.[30]

Transmission Electron Microscopy. The catalyst particle size and morphology were examined by bright-field and dark-

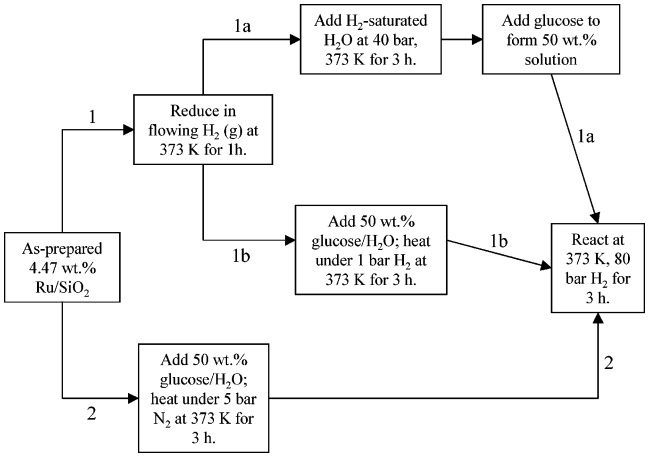

Figure 4. Schematic diagram representing kinetic studies performed under various pretreatments.

field transmission electron microcopy (TEM), selected-area electron diffraction (SAED), and high-resolution TEM (HR-TEM) using a JEOL 2010F analytical electron microscope (AEM) equipped with a Schottky field-emission (FE) gun and a high-tilt pole piece (spherical aberration coefficient of Cs = 1.0 mm and 0.23 nm point-to-point resolution) and operated at 200 kV. Energy-dispersive X-ray spectroscopic (EDXS) analyses were performed with a JEOL 2010F FE-AEM, which has an Oxford Instruments ultrathin-window EDX detector with a 136 eV resolution at the Mn Kα line (5.9 keV) and nanoprobe capabilities with a probe diameter varying from 2.4 to 0.5 nm. Samples were tilted 15° toward the detector. The samples were supported on copper mesh microscopy grids with holey carbon films by dipping the grid into the catalyst powder and shaking the excess. Ruthenium particle size distributions both for the as-prepared 4.47 wt % Ru/SiO_2 catalyst and the same catalyst recovered after hydrogenation were determined using the ImagePro software, version 5.1 (Media Cybernetics, Inc., Silver Spring, MD).

Adsorption of H_2. The ruthenium dispersion and particle size of the Ru/SiO_2 catalysts were determined by H_2 chemisorption performed on a Coulter Omnisorp3 100CX instrument at 303 K in the pressure range 0−150 Torr. Prior to chemisorption, the catalysts were heated from ambient conditions to 648 K at 4 K min^{-1} in flowing H_2 (BOC 99.999%). The catalysts were reduced in H_2 at 648 K for 75 min prior to cooling to 303 K. Surface Ru was evaluated by the total amount of H_2 adsorbed at 303 K extrapolated to zero pressure, assuming a stoichiometry ratio (H/Ru) equal to unity.

Hydrogenation Procedure. The hydrogenation of glucose to sorbitol was carried out in a 50 mL Parr Instrument Company 4592 batch reactor. In the standard reaction, 30 mL of a 50 wt % aqueous glucose (Alfa Aesar, 99%) stock solution was loaded into the reactor along with 0.05 g (particle size 53−180 μm) of the as-prepared catalyst. The reactor was fitted with a dip tube and a 10 μm stainless steel filter to allow for periodic liquid sampling of the reaction mixture. To remove air in the headspace, N_2 (BOC, 99.998%) was bubbled through the reactor for 30 min at ambient temperature. The vessel was then sealed and heated at a rate of 2 K min^{-1} to 373 K. After reaching 373 K, the vessel was flushed three times with 5 bar H_2 to remove the N_2. A liquid sample was removed from the vessel immediately after flushing to mark the start of the reaction. After sampling, H_2 was added to a total pressure of 80 bar and the reactor was stirred for 3 h. Samples of the reaction mixture were removed periodically to track the progress of the hydrogenation.

TABLE 1: Comparison of the Reaction Rates Observed after the Various Pretreatments to the Standard Rate of Hydrogenation over a 4.47 wt % Ru/SiO_2 Catalyst

path	rate ($mol_{sorbitol\ produced}(mol_{total\ Ru})^{-1}\ s^{-1}$)
standard reaction	0.17 ± 0.02
1a	0.09 ± 0.03
1b	0.13 ± 0.01
2	0.08 ± 0.01

During the reaction, consumption of H_2 resulted in a decrease in pressure of up to 20 bar; however, following the periodic sampling of the reactor contents, the pressure was returned to 80 bar using H_2. Upon completion of the reaction, the vessel was allowed to cool to ambient temperature and the pressure was released. Product solutions were filtered through a series of Pall Gelman 0.45 and 0.20 μm syringe filters. The filtrate was analyzed by either a Waters, model 501, High Performance Liquid Chromatograph (HPLC) or a Waters, model 717, plus Autosampler HPLC equipped with a Waters, model R401, differential refractometer. Both an Aminex fermentation monitoring column (Bio-Rad) and an Aminex HPX-87H column (Bio-Rad) were used for separation of the products. The columns and refractive index detector were maintained at 333 and 304 K, respectively. The mobile phase consisted of 5 mM sulfuric acid at a flow rate of 0.5 mL min^{-1}.

Results and Discussion

To explore the stability of Ru/SiO_2 catalysts during the aqueous phase hydrogenation of glucose, three different techniques were employed. In the first, a 4.47 wt % Ru/SiO_2 catalyst was subjected to various pretreatments after which the pretreated catalysts were used for a hydrogenation reaction. The global rate of hydrogenation was measured over these pretreated catalysts and compared to the rate over an untreated catalyst during the standard hydrogenation reaction described in the Experimental Section. In a second technique, in situ X-ray absorption spectroscopy was used to monitor how the pretreatment conditions employed during the kinetic studies affect the Ru oxidation state and particle size. Last, transmission electron microscopy was used to visually track changes in the catalyst before and after use in a standard hydrogenation reaction.

Pretreatment Studies. As summarized in Figure 4, these pretreatments probed the influence of initial Ru oxidation state and aqueous environment on the rate of hydrogenation (moles of sorbitol produced(total moles of Ru)$^{-1}$ s^{-1}). Comparison of paths 1a and 1b to path 2 examines the effect of initial Ru oxidation state on the rate of glucose hydrogenation. Comparison of paths 1b and 2 to path 1a tests the effect of glucose in the aqueous medium during pretreatment. In paths 1b and 2, the catalyst was pretreated in a glucose/water solution for 3 h prior to hydrogenation. In path 1a, the aqueous pretreatment involves only H_2-saturated water. The reaction rates observed after the various pretreatments are compared to that observed during the standard hydrogenation reaction, which was 0.17 ± 0.02 $mol_{sorbitol\ produced}(mol_{total\ Ru})^{-1}\ s^{-1}$ over a 4.47 wt % Ru/SiO_2 catalyst. As reported in Table 1, the various pretreatments lowered the rate of glucose hydrogenation per Ru metal atom. The rates of reaction after pretreating the catalysts along paths 1a and 2 were nearly half that of the standard reaction, which suggests that the pretreatment conditions lowered the availability of active Ru by half.

In some cases, an induction period was observed in the conversion of glucose with time, as depicted in Figure 5. The induction period was clearly observed for the pretreatment described in path 2. As the pretreatment conditions appear to alter the availability of Ru on the silica surface, which may

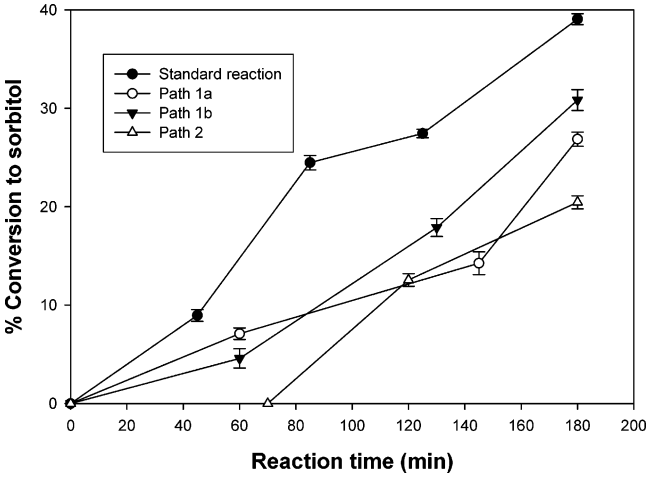

Figure 5. Conversion of glucose to sorbitol over 4.47 wt % Ru/SiO_2 at 373 K and 80 bar H_2 following the pretreatment paths shown in Figure 4. The error bars represent 95% confidence limits.

result in the observed induction periods, detailed XAS studies were used to explore the influence of pretreatments on the state of the Ru.

X-ray Absorption Spectroscopy. In situ XAS studies were performed in a high-pressure cell to mimic the conditions of the pretreatment paths in Figure 4. Figure 6 presents the X-ray absorption near edge structure (XANES) of the 4.47% Ru/SiO_2 catalyst before and after various pretreatments. In addition, spectra of RuO_2 and large clusters of Ru/Al_2O_3 (17.6 wt %) were used as references.

The X-ray absorption near edge spectra in Figure 6 confirm that Ru is oxidized on the as-prepared 4.47 wt % Ru/SiO_2 sample exposed to air. Treatment of the sample in H_2 at 373 K reduced the Ru to metal particles in the presence or absence of liquid water. Reduction was also accomplished by H_2 in a glucose/water mixture. Thus, the chemical state of Ru during the hydrogenation reaction is metallic, regardless of the pretreatment conditions. Nevertheless, the induction period observed after pretreatment path 2 suggests a slow reduction process after prolonged exposure to the glucose/water solution.

The extended X-ray absorption fine structure (EXAFS) associated with each of the spectra shown in Figure 6 was analyzed to determine the Ru coordination number (N), Ru−Ru interatomic distance (R), change in Debye−Waller factor ($\Delta\sigma^2$), and shift in edge energy (ΔE_0). The Fourier transforms of the EXAFS are given in Figure 7. EXAFS parameters derived from curve fitting are provided in Table 2. The $\Delta\sigma^2$ value was calculated relative to the metallic Ru/Al_2O_3 reference.

A plausible explanation for the decrease in the global hydrogenation rate with treatment in water at 373 K is a decrease in the availability of surface Ru. Analysis of the Ru K edge EXAFS of 4.47 wt % Ru/SiO_2 reduced by H_2(g) at 373 K revealed a Ru−Ru coordination number of 8.9 (Table 2), which corresponds to an average spherical particle size of 1.5−2.5 nm. However, when H_2-saturated water at 373 K and 40 bar was added to the reduced catalyst, the coordination number increased to 11, indicating substantial particle growth. The EXAFS results summarized in Table 2 show that particle growth in water occurred regardless of the initial Ru oxidation state. Interestingly, the presence of glucose in the water inhibited particle growth. The as-prepared catalyst treated at 373 K with H_2-saturated glucose/water solution revealed a coordination number of 8.6, which is similar to the sample reduced by H_2(g) at 373 K. However, a sample prereduced with H_2(g) and then

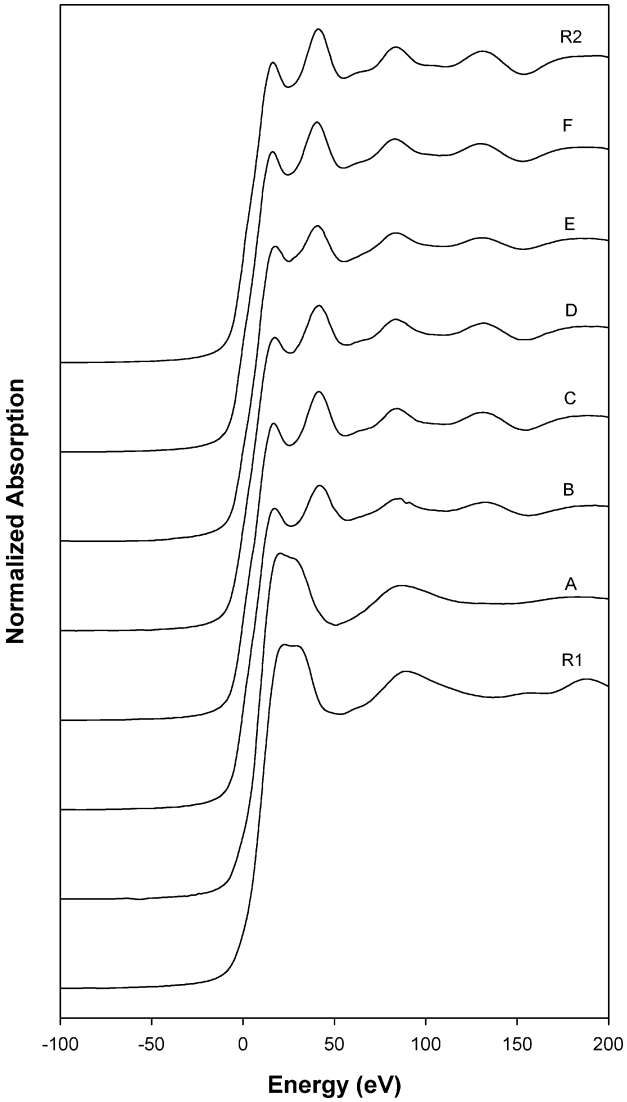

Figure 6. X-ray absorption near edge spectra of 4.47 wt % Ru/SiO_2 at the Ru K edge: (R1) RuO_2 reference; (A) as-prepared catalyst; (B) reduced in H_2(g); (C) reduced in H_2(g) followed by the addition of H_2-saturated H_2O; (D) as-prepared catalyst reduced by H_2-saturated H_2O; (E) as-prepared catalyst reduced by the addition of H_2-saturated glucose/H_2O; (F) reduced in H_2(g) followed by the addition of H_2-saturated glucose/H_2O; (R2) Ru/Al_2O_3 reference. The spectra are offset for clarity. The energies are defined relative to the first inflection point of the Ru/Al_2O_3 (R2) sample.

exposed to H_2-saturated glucose/water solution had a coordination number of 10, which is consistent with some particle growth that is not as severe as a treatment in H_2-saturated water. Evidently, aqueous phase glucose helps stabilize the oxidized Ru from sintering into large metal particles upon reduction.

During the standard hydrogenation procedure, the as-prepared catalyst was not prereduced prior to the addition of glucose/water solution. Therefore, the highest global reaction rate obtained with this procedure is the direct result of higher Ru dispersion on the support. The various pretreatment conditions facilitate particle growth and decreased availability of surface Ru, which leads to lower global reaction rates.

Transmission Electron Microscopy. To complement the XAS studies, TEM was used to monitor the size and distribution of Ru particles on one sample before and after use in the hydrogenation reaction. Parts a and b of Figure 8 show micrographs of the 4.47 wt % Ru/SiO_2 catalyst as prepared and recovered by filtration after a standard hydrogenation reaction,

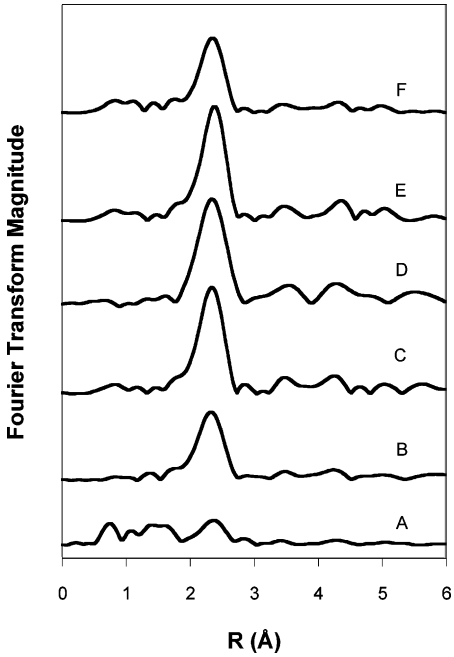

Figure 7. Magnitude of the radial distribution function (not corrected for phase shifts) after Fourier transformation (k^3 weighting) for the 4.47 wt % Ru/SiO_2 under various aqueous pretreatments: (A) as-prepared catalyst; (B) reduced in H_2(g); (C) reduced in H_2(g) followed by the addition of H_2-saturated H_2O; (D) as-prepared followed by the addition of H_2-saturated H_2O; (E) reduced in H_2(g) followed by the addition of H_2-saturated glucose/H_2O; (F) as-prepared reduced by the addition of H_2-saturated glucose/H_2O. The transforms are offset for clarity.

TABLE 2: Summary of the First-Shell Ru−Ru Coordination Number (*N*), Ru−Ru Interatomic Distance (*R*), Change in Debye−Waller Factor ($\Delta\sigma^2$) Relative to Metallic Ru/Al_2O_3, and Shift in Edge Energy (ΔE_0) Obtained for the Catalysts under Various Treatments[a]

treatment	*N*	*R* (Å)	$\Delta\sigma^2$ (Å^2)	ΔE_0 (eV)
A	3.7	2.68	0.0042	2.8
B	8.9	2.66	0.0032	−1.4
C	11	2.68	0.0018	0.9
D	11	2.68	0.0014	0.5
E	10	2.68	0.0019	−1.6
F	8.6	2.67	0.0031	−2.2
G	9.5	2.66	0.0021	−2.7
H	9.3	2.65	0.0032	−1.0

[a] (A−F) 4.47 wt % Ru/SiO_2; (G and H) 12.98 wt % Ru/C_{ex}. (A) As-prepared catalyst; (B) reduced in H_2(g); (C) reduced in H_2(g) followed by the addition of H_2-saturated H_2O; (D) as-prepared reduced by the addition of H_2-saturated H_2O; (E) reduced in H_2(g) followed by the addition of H_2-saturated glucose/H_2O; (F) as-prepared reduced by the addition of H_2-saturated glucose/H_2O; (G) as-prepared Ru/C reduced in H_2(g); (H) as-prepared Ru/C reduced in 40 bar H_2-saturated H_2O. All XAS data were collected at 373 K, except for samples A and G, which were collected at 298 K.

respectively. Shown beside the micrographs are the corresponding differential histograms of Ru particle size, which match well to a normal distribution curve. For the as-prepared catalyst, the size of fairly well dispersed rounded particles varied from 1.6 to 4.8 nm with a mean roundness of 1.18. In a typical aggregate formed during hydrogenation, as shown in Figure 8b, the particle sizes were slightly higher, varying from 1.9 to 5.4 nm with a mean roundness of 1.12. However, in both cases, the mean of the particle size was estimated as 3.0 ± 0.1 nm. Although the SiO_2 support could mask to some extent the contrast arising from ultrafine Ru particles, dark-field TEM observations (diffraction contrast) in conjunction with SAED and HRTEM (phase contrast) indicated their crystallinity. Thus, the enlarged upper right inset in Figure 8b shows 0.23 nm (100) hcp Ru lattice fringes of the aggregated metal particles. EDXS analyses of individual 3−5 nm Ru particles performed using 0.5−2.4 nm diameter electron probes in randomly chosen areas of both the as-prepared catalyst and the catalyst after hydrogenation showed that the particles were highly pure, with no impurities or admixtures.

Although Ru particle growth was not observed in the EXAFS for an as-prepared catalyst treated with H_2-saturated glucose/water solution, severe restructuring of the catalyst was observed by TEM. Figure 8a shows the as-prepared 4.47 wt % Ru/SiO_2 sample with well-distributed Ru particles on the silica support with a mean particle size of about 3.0 ± 0.1 nm. After reaction, the mean Ru particle size was essentially unchanged, but the distribution of Ru was severely altered. The sample appears to contain large aggregate regions of high Ru particle density. Although glucose/water solution inhibited particle growth as determined by EXAFS, the metal particles were clearly mobile on the support, which suggests a poor long-term stability of the catalyst under these reaction conditions.

Sintering of supported metal catalysts is usually viewed as occurring by one of the following mechanisms: (1) migration of crystallites on the surface of the support, (2) migration of atomic species on the support, and (3) dissolution and redeposition of metal ions.[31] The first two mechanisms are commonly considered with high-temperature reactions, while the third mechanism occurs in liquid phase reactions at relatively low temperatures. The results obtained in this work support the findings of Hoang et al., who showed that sintering of silica-supported Ru catalysts occurred in liquid water under 60 bar H_2 at 373 K in an autoclave reactor.[27] They found that Ru particles of varying initial dispersions (15−86%) sintered to a final dispersion of ∼10% after 4 h in liquid water and speculated that the mechanism for agglomeration was the formation of a soluble $Ru(OH)_x$ species that readsorbed and reduced on larger Ru particles. Because of the flow-through design of the XAS cell used in our work, it is expected that a percentage of the soluble species would eventually be washed out of the catalyst bed before readsorbing to form larger particles. By tracking the X-ray absorption coefficient (which is directly proportional to the amount of Ru present) during the XAS experiments, it is possible to monitor the Ru content. Analysis of all of the progressive scans during each aqueous treatment showed no decrease in the $\Delta\mu x$ value at the Ru K edge. This finding suggests that sintering did not occur via a soluble species but more likely occurred by migration of the Ru during hydrolysis of the silica. Indeed, Hoang et al. report a loss of silica surface area by treatment in water.[27] Inspection of the histograms shown in Figure 8 reveals that the average Ru particle size did not change over the course of the reaction. Instead, Ru particles appeared to migrate on the surface of the silica to regions of higher particle density. This migration occurred over the course of a 3 h hydrogenation reaction. One could imagine that, given additional exposure to the glucose/water solution, the Ru particles would coalesce to form larger particles. This theory is supported by the behavior of path 2 in Figure 4. After the initial induction period, the rate of hydrogenation appears to be comparable to that of the standard hydrogenation reaction. This suggests that Ru particles coalesced during the extended glucose/water treatment, subsequently taking a longer time to reduce. In fact, when the hydrogenation reaction was conducted over a period of 6 h using half the amount of catalyst compared to the standard reaction, the resulting overall rate of reaction was 0.08 $\pm$ 0.01 $mol_{sorbitol\ produced}(mol_{total\ Ru})^{-1}\ s^{-1}$. This overall rate

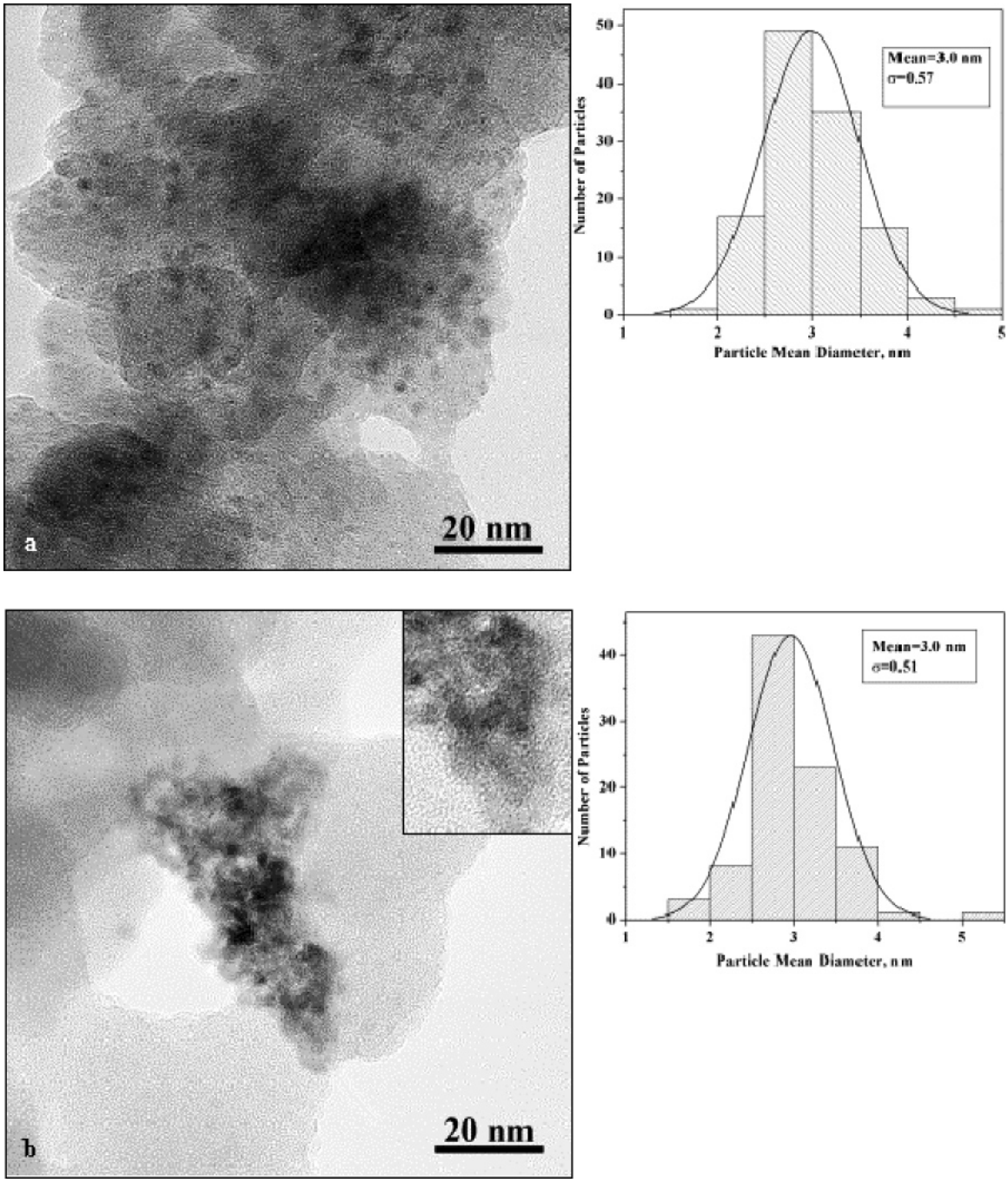

Figure 8. High-magnification TEM images of 4.47 wt % Ru/SiO_2 with the corresponding histograms of Ru particle size: (a) as-prepared catalyst; (b) after standard hydrogenation reaction, demonstrating changes in the surface distribution and aggregation of 3 nm Ru particles. The aggregate contains about 90 particles. The enlarged upper right inset in part b shows (100) hcp Ru lattice fringes. Continuous lines in histograms denote normal distribution curves.

matches that observed after the pretreatment of path 2 in Figure 4, further supporting the conclusion that coalescence of Ru particles can eventually lead to sintering of these particles. The TEM and XAS studies in combination with the kinetics studies suggest that sintering of Ru particles occurred via the migration of crystallites on the support.

To explore the effect of support on the stability of Ru particles under aqueous phase reaction conditions, a carbon-supported Ru sample was also examined by XAS. Table 2 contains the structural properties of Ru/C that was reduced in either gaseous H_2 at 373 K or H_2-saturated liquid water at 373 K and 40 bar total pressure. The Ru−Ru coordination number remained essentially unchanged during these treatments, indicating that Ru particle growth did not occur on the carbon-supported samples. This also supports the conclusion that there was no dissolution and redeposition of Ru ions under the aqueous conditions. Furthermore, kinetic studies on a separate commercial Ru/C (Acros, 5 wt % Ru) catalyst show that, contrary to the Ru/SiO_2 catalyst, the rate of hydrogenation does not decrease with extended reaction time. The overall rate of the standard hydrogenation was 0.12 ± 0.02 and 0.11 ± 0.01 $mol_{sorbitol\ produced}(mol_{total\ Ru})^{-1}\ s^{-1}$ after 3 and 6 h of reaction, respectively. This indicates that Ru particles are more stable on a carbon support and less likely to sinter under aqueous phase reaction conditions when compared to the silica-supported counterparts.

As sintering of Ru particles occurred on the silica-supported sample but not on the carbon-supported sample, we concluded

TABLE 3: Results of H_2 Chemisorption Providing an Estimate of Ru Dispersion and Particle Size

catalyst	Ru wt %	dispersion (%)	particle size[a] (nm)	TOF[b] (s^{-1})
Ru/SiO_2	0.56	91	1.1	0.28 ± 0.02
Ru/SiO_2	2.67	78	1.3	0.21 ± 0.04
Ru/SiO_2	4.47	53	1.9	0.32 ± 0.13
Ru/C[c]	5[d]	43	2.4	0.25 ± 0.03

[a] Estimated from H_2 chemisorption (1/dispersion). [b] TOFs given with 95% confidence intervals. [c] Commercial catalyst purchased from Acros Organics. [d] Ru loading provided by Acros Organics.

that particle growth depends on catalyst support, not catalyst metal. Similar results have been found for supported Pt catalysts. Douidah et al. compared the stability of silica- and alumina-supported Pt catalysts under H_2 in the aqueous phase at varying pH.[32] They found a decrease in Pt dispersion on the silica but not on the alumina following an aqueous treatment. It was concluded that, on the silica-supported catalysts, the loss of metal dispersion was due to Pt particle growth. In a study of small Ru particles deposited on a variety of supports, it was found that the strength of the metal−support interaction was inversely proportional to the electronegativity of the support metal ion.[33] A strong interaction between the support metal and support oxygen results in a weak interaction between the Ru metal and the support oxygen, resulting in a weakly anchored catalyst. In a similar study, small Ru particles were prepared on a range of supports that were analyzed with XAS.[34] Analysis of the distance of the Ru to support oxygen showed that the Ru−O distance for silica was longer than those for Ru supported on alumina and magnesia. Treating the bond distance as being inversely proportional to the bond strength would indicate that the silica-supported catalyst is more weakly anchored on the silica support compared to the alumina and magnesia supports. The results presented in this work are in agreement with the idea that Ru particles are weakly anchored to the silica support. The XAS studies have shown that the addition of glucose to the reaction media slowed the rate of particle growth on the Ru/SiO_2 catalyst. The mechanism by which glucose stabilizes the catalyst is not known but is the subject of further study.

As the presence of glucose stabilizes the Ru particles on the as-prepared Ru/SiO_2 catalyst, a true kinetic study of the use of these catalysts in glucose hydrogenation was feasible. A series of three silica-supported catalysts was prepared with different Ru loadings; Table 3 summarizes the Ru loading and dispersion determined from H_2 chemisorption for each of the samples. The inverse of the dispersion provides a simple estimate for the mean Ru particle size.[35] As shown in Table 3, an increase in Ru loading corresponded to a decrease in Ru dispersion.

The primary tool for characterization of these catalyst samples was H_2 chemisorption, as shown in Table 3. However, EXAFS analysis and TEM studies were used to corroborate the H_2 chemisorption results for the 4.47 wt % Ru/SiO_2 catalyst. A Ru particle size of 1.9 nm was estimated by H_2 chemisorption, which is in fair agreement with the estimate of 3.0 ± 0.1 nm obtained by TEM. Following reduction of the catalyst in H_2-(g), the EXAFS analysis yielded a Ru coordination number of 8.9 (Table 2) which corresponds to an average spherical particle size of about 1.5−2.5 nm.[36] Agreement between the results of H_2 chemisorption, TEM, and EXAFS analysis indicates that H_2 chemisorption is an appropriate tool for the estimate of Ru particle size.

As shown in Figure 9, the conversion of glucose to sorbitol was linear with time over the first 3 h. The average turnover frequency (TOF) for glucose hydrogenation is presented in Table 3 for each of the catalysts. The Ru/SiO_2 tested in our work had

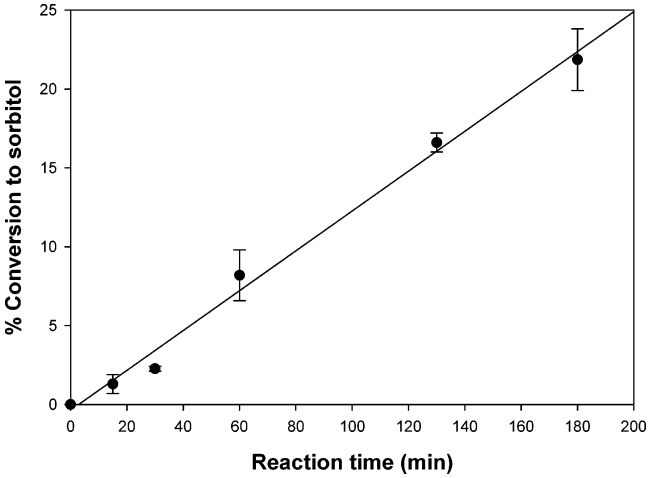

Figure 9. Percent conversion of glucose to sorbitol over Ru/SiO_2 (2.67 wt %) as a function of time at 373 K and 80 bar H_2. The line represents a linear regression of the data. The error bars represent 95% confidence limits.

the same TOF as Ru/C (Acros), which is among the highest reported in the literature. Gallezot et al. studied the hydrogenation of glucose to sorbitol over a 1.6 wt % Ru/C catalyst in a trickle-bed reactor under similar reaction conditions of 373 K and 80 bar H_2 pressure.[26] Assuming 100% dispersion of Ru based on TEM results, the authors reported a TOF of 0.03 s^{-1}. The lower TOF obtained by Gallezot et al. may be due to internal mass transfer limitations. Kusserow et al. studied the batchwise hydrogenation of glucose over a 2.75 wt % Ru/Al_2O_3 catalyst at 393 K and 120 bar H_2 pressure.[15] On the basis of a Ru particle size of 1.0 nm, as determined by TEM (100% dispersion), the TOF for glucose hydrogenation was approximately 0.08 s^{-1}.

The Madon−Boudart criterion was applied in our study to determine if mass transfer artifacts in the kinetic data were significant during the hydrogenation reaction.[37] Thus, glucose hydrogenation was performed over a series of silica-supported catalysts with various Ru loadings. As shown in Table 3, the concentration of Ru varied by nearly an order of magnitude, while the Ru dispersion changed by only a factor of 2. The turnover frequency of the hydrogenation reaction was nearly constant over this series of catalysts, which, according to the Madon−Boudart criterion, indicates that mass transfer artifacts are negligible in this system. Thus, the rate of hydrogenation should be a good measure of available surface Ru atoms in the reactor.

Conclusions

This work has shown that, in the presence of H_2-saturated water, silica-supported Ru catalysts were unstable due to sintering of the Ru particles. This sintering occurred regardless of the initial Ru oxidation state. When the catalyst was reduced prior to treatment with a H_2-saturated glucose/water solution, there was also growth of Ru particles. However, the extent of particle growth did not appear as significant as that in a purely aqueous environment. The presence of glucose in a H_2-saturated aqueous solution appeared to stabilize initially oxidized Ru particles against sintering. These findings were important, as they closely mimicked the conditions for the standard hydrogenation reaction. Transmission electron microscopy confirmed that Ru particles did not sinter during glucose hydrogenation; however, there was migration of the Ru, forming regions of higher particle density. Comparison of the XAS and TEM

studies with the kinetic studies suggests that glucose can only stabilize Ru against sintering for a limited period of time (~3 h as performed in these studies). Extended exposure (~6 h) of the Ru/SiO_2 catalyst to aqueous conditions resulted in growth of Ru particles and consequently a reduced rate of glucose hydrogenation. It is likely that the mechanism of particle growth involves migration of Ru species during the hydrolysis of the silica surface. While Ru-based catalysts are effective hydrogenation catalysts, supports other than silica should be considered for the aqueous phase hydrogenation of glucose.

Acknowledgment. This work was supported by the National Science Foundation (CTS-0313484). Research was carried out in part at the National Synchotron Light Source, Brookhaven National Laboratory, which is supported by the U.S. Department of Energy, Division of Materials Sciences and Division of Chemical Sciences, under Contract No. DE-AC02-98CH10886. V.O. gratefully acknowledges the support by the Director, Office of Science, Division of Materials Science & Engineering, U.S. Department of Energy, under Contract No. DE-FG02-01ER45918.

References and Notes

(1) Cortright, R. D.; Davda, R. R.; Dumesic, J. A. *Nature* **2002**, *418*, 964.
(2) Davda, R. R.; Dumesic, J. A. *Angew. Chem., Int. Ed.* **2003**, *42*, 4068.
(3) Davda, R. R.; Shabaker, J. W.; Huber, G. W.; Cortright, R. D.; Dumesic, J. A. *Appl. Catal., B* **2005**, *56*, 171.
(4) Huber, G. W.; Cortright, R. D.; Dumesic, J. A. *Angew. Chem., Int. Ed.* **2004**, *43*, 1549.
(5) Huber, G. W.; Shabaker, J. W.; Dumesic, J. A. *Science* **2003**, *300*, 2075.
(6) Embree, H. D.; Chen, T.; Payne, G. F. *Chem. Eng. J.* **2001**, *84*, 133.
(7) Cortright, R. D.; Sanchez-Castillo, M.; Dumesic, J. A. *Appl. Catal., B* **2002**, *39*, 353.
(8) Chen, N. Y.; Degnan, T. F.; Koenig, L. R. *CHEMTECH* **1986**, 506.
(9) Hollingsworth, R. I. *Chem. Eng.* **2001**, 66.
(10) Ritter, S. K. *Chem. Eng. News* **2004**, *82*, 31.
(11) Lichtenthaler, F. W.; Mondel, S. *Pure Appl. Chem.* **1997**, *69*, 1853.
(12) Crezee, E.; Hoffer, B. W.; Berger, R. J.; Makkee, M.; Kapteijn, F.; Moulijn, J. A. *Appl. Catal., A* **2003**, *251*, 1.
(13) Tronconi, E.; Ferlazzo, N.; Forzatti, P.; Pasquon, I.; Casale, B.; Marini, L. *Chem. Eng. Sci.* **1992**, *47*, 2451.
(14) Phillips, M. A. *Br. Chem. Eng.* **1963**, *8*, 767.
(15) Kusserow, B.; Schimpf, S.; Claus, P. *Adv. Synth. Catal.* **2003**, *345*, 289.
(16) Turek, F.; Chakrabarti, R. K.; Lange, R.; Geike, R.; Flock, W. *Chem. Eng. Sci.* **1983**, *38*, 275.
(17) Dechamp, N.; Gamez, A.; Perrard, A.; Gallezot, P. *Catal. Today* **1995**, *24*, 29.
(18) Gallezot, P.; Cerino, P. J.; Blanc, B.; Fleche, G.; Fuertes, P. *J. Catal.* **1994**, *146*, 93.
(19) Li, H.; Wang, W.; Fa Deng, J. *J. Catal.* **2000**, *191*, 257.
(20) Li, H.; Li, H.; Deng, J. F. *Catal. Today* **2002**, *74*, 53.
(21) Wisniak, J.; Simon, R. *Ind. Eng. Chem. Prod. Des. Dev.* **1979**, *18*, 50.
(22) Li, H.; Li, H.; Wang, M. *Appl. Catal., A* **2001**, *207*, 129.
(23) Li, H.; Deng, J.-F. *J. Chem. Technol. Biotechnol.* **2001**, *76*, 985.
(24) van Gorp, K.; Boerman, E.; Cavenaghi, C. V.; Berben, P. H. *Catal. Today* **1999**, *52*, 349.
(25) Arena, B. J. *Appl. Catal., A* **1992**, *87*, 219.
(26) Gallezot, P.; Nicolaus, N.; Fleche, G.; Fuertes, P.; Perrard, A. *J. Catal.* **1998**, *180*, 51.
(27) Hoang, L. C.; Menezo, J. C.; Montassier, C.; Barbier, J. *Bull. Soc. Chim. Fr.* **1991**, *128*, 491.
(28) Bowron, D. T.; Weigel, R.; Filipponi, A.; Roberts, M. A.; Finney, J. L. *Mol. Phys.* **2001**, *99*, 761.
(29) Ressler, T. *WinXAS*, version 2.33, 2001; www.winxas.de.
(30) Koningsberger, D. C.; Mojet, B. L.; Dorssen, G. E. v.; Ramaker, D. E. *Top. Catal.* **2000**, *10*, 143.
(31) Besson, M.; Gallezot, P. *Catal. Today* **2003**, *81*, 547.
(32) Douidah, A.; Marecot, P.; Barbier, J. *Appl. Catal., A* **2002**, *225*, 11.
(33) Asakura, K.; Iwasawa, Y. *J. Chem. Soc., Faraday Trans.* **1990**, *86*, 2657.
(34) Mizushima, T.; T., K.; Udagawa, Y.; Ueno, A. *J. Am. Chem. Soc.* **1990**, *112*, 7887.
(35) Boudart, M.; Djega-Mariadassou, G. *Kinetics of Heterogeneous Catalytic Reactions*; Princeton University Press: Princeton, NJ, 1984.
(36) Greegor, R. B.; Lytle, F. W. *J. Catal.* **1980**, *63*, 476.
(37) Madon, R. J.; Boudart, M. *Ind. Eng. Chem. Fundam.* **1982**, *21*, 438.